International Journal of Infrared and Millimeter Waves, Vol. 14, No. 12, 1993

MICROWAVE CAVITY PERTURBATION TECHNIQUE: PART II: EXPERIMENTAL SCHEME

Steve Donovan,* Olivier Klein,† Martin Dressel, Károly Holczer, and George Grüner

Department of Physics and Solid State Science Center
University of California, Los Angeles
Los Angeles, California 90024-1547

Received September 22, 1993

Abstract

In this paper, the second in a three part series, we describe an experimental scheme used to measure the electrodynamical response of a material in the millimeter wave range of frequency. In particular, with this technique we can directly evaluate the complex conductivity from a measurement of *both* the bandwidth and characteristic frequency of a resonator containing the specimen. We will describe in detail all the technical improvements achieved which provide the required accuracy.

Keywords: millimeter wave measurement, cavity perturbation technique, cavity design, microwave setup, experimental procedure

1 Introduction

The experimentalist interested in spectroscopically exploring the microwave and millimeter spectral range (3-300 GHz) is faced with a variety of challenges. The origin of these difficulties in this spectral range stems primarily from two different effects:

*present address: Max-Planck-Institut für Festkörperforschung, Heisenbergstr. 1, D 70569 Stuttgart, Germany

†present address: Physics Department, Massachusetts Institute of Technology, 77 Massachusetts Ave., Cambridge MA 02139

0195-9271/93/1200-2459$07.00/0

1. Sources, detectors and all other components used in this frequency range have a limited bandwidth and are usually considered to be "broad band" if they cover a 10% range around their central frequency.

2. The wavelengths in this region (wavelength of 1.0 mm to 100 mm) are comparable to most laboratory-sized devices and therefore diffraction effects are non-negligible.

The large diffraction effects essentially rule out the possibility of any type of conventional optical spectroscopy. Furthermore, the severe bandwidth limitations practically necessitate the use of a different set of instruments at each desired frequency. One is then left to piece together a spectrum from a variety of measurements made with a collection of different instruments. However, the disadvantages associated with the incomplete frequency coverage can be partially compensated for by the use of different resonant techniques and narrow band detection schemes to achieve a much higher relative sensitivity than with conventional spectroscopic techniques. This is particularly important when studying highly conducting materials whose reflectivity at these frequencies is already very close to 100%.

The most common technique used to measure the conductivity in this frequency range is the so-called cavity perturbation technique. In this technique, a small sample is introduced into a resonant cavity of quality factor Q. The change in the cavity characteristics (i.e. the resonant frequency $\omega_o/2\pi$ and the width of the resonance Γ) due to the introduction of the sample under investigation are measured and a direct evaluation of the complex conductivity $\hat{\sigma} = \sigma_1 + i\sigma_2$ is possible provided one measures *two* independent parameters. Unfortunately, with most of the commonly used techniques one typically measures f_o to a precision which is one order of magnitude smaller than Γ. This is particularly problematic when measuring highly conducting samples whose dimensions exceed their skin depth δ. In this case, $\hat{\sigma}$ is determined in part by the small frequency deviation from an identically shaped perfect conductor, and the small relative effect coupled with the large frequency measurement uncertainty prevents a direct evaluation of $\hat{\sigma}$.

The situation is analogous to that encountered in a standard optical measurement, where a measurement of the two independent variables, the phase and amplitude of the reflectivity (or transmission), is not generally possible. In this case, one normally takes advantage of the fact that the reflectivity can be measured over a very broad spectral range, and thereby, from arguments of causality (together with a suitable frequency extrapolation), one

can invoke the Kramers-Kronig relations to determine the other unmeasured parameter [1]. In this way one indirectly evaluates $\hat{\sigma}$.

By combining the one parameter measured in the micro and millimeter wave range ($\Delta\Gamma$) together with optical data, one can also indirectly determine $\hat{\sigma}$ in this range. However, the errors introduced by such an analysis are difficult to estimate and it is certainly preferable to be able to directly evaluate the conductivity. In this report we will describe in detail experimental methods which allow for the evaluation of $\hat{\sigma}$ by directly measuring *both* characteristics f_o and Γ with nearly equal precision.

We will describe in some detail several important parameters to consider when designing a microwave cavity perturbation experiment. We will then describe both the standard cavity technique together with the modifications which allow for a measurement of both the bandwidth and the characteristic frequency with a relative accuracy better than 1 ppm. We will discuss the principles of operation while trying to emphasize the relevant characteristics of the components which directly influence the end performance. Finally, we describe the analysis required to extract f_o and Γ from the measured parameters using the so-called amplitude technique.

2 Design Considerations

In a cavity perturbation experiment one measures the change in width Γ and frequency ω_o of a resonant structure which occur due the introduction of a foreign body. Provided the perturbation is suitably small, one can determine the material properties of the body from the measured changes in the cavity characteristics (see Part I [2]). The cavity perturbation equation is

$$\Delta\hat{\omega} = -4\pi\gamma\hat{\alpha} \tag{1}$$

where $\hat{\omega} = \omega_o - i\Gamma/2Q$, γ is a constant which is proportional to the sample to cavity volume ratio times a constant which depends (weakly) on the field configuration (mode) within the cavity, and $\hat{\alpha}$ is the sample polarizability.

The most important conditions pertaining to the cavity which must be satisfied in order for such an analysis to hold are:

1. $\lambda > 2a$, where λ is the wavelength of the electromagnetic radiation and $2a$ the largest sample dimension.

2. $V_s/V_c \ll 1$, where V_s and V_c are the sample and cavity volumes, respectively.

3. The field distribution must be known in order to determine the absolute value of the conductivity of the body.

The measurement sensitivity S is ultimately determined by the ratio

$$S = \frac{\Delta\Gamma}{\Gamma}, \tag{2}$$

and in order to maximize S, both the maximum $\Delta\Gamma$ and minimum Γ are desired. Apart from a factor of V_s/V_c, $\Delta\Gamma$ is only weakly dependent on the particular mode of the resonator, and we will therefore concentrate on cavity design considerations which will maximize the Q subject only to the constraint that V_c should be minimized.

2.1 The Resonator

The most practical means of developing a high frequency, high Q resonator is to enclose the fields within a body whose dimensions are comparable to the desired wavelength of operation. Such a device is normally referred to as a resonant cavity, and it will support a series of modes, with a lower cut-off, each corresponding to a unique distribution of fields. Most resonators are fabricated out of highly conducting (or superconducting) material and in this case the fields are determined solely by the boundary conditions at the interior surfaces. For ease of fabrication, one is generally limited to cylindrical or rectangular cavities, and in these cases one can easily determine the field distribution within the resonator. For a given measurement frequency, the minimum cavity dimensions are roughly given by 1/2 the wavelength in each physical dimension.

The Q of the cavity is determined by the energy loss per cycle and there are three main loss mechanisms: Ohmic losses in the cavity walls, radiative losses in the coupling device, and losses within the sample placed in the cavity. These different mechanisms contribute in an additive way and the total loss is determined by the sum of the reciprocals of the Q related to each loss mechanism,

$$\frac{1}{Q} = \frac{1}{Q_u} + \frac{1}{Q_r} + \frac{1}{Q_s} \tag{3}$$

where Q represents the total, or loaded, cavity loss, Q_u the Ohmic, or unloaded, loss, Q_r the radiative loss, and Q_s the sample loss.

Apart from a constant on the order of unity (determined by the particular mode), Q_u is given by the ratio of the volume occupied by the fields to the volume of the conductor into which the fields penetrate [3]

$$Q_u = \frac{V_c}{A\delta}, \tag{4}$$

where A is the total interior surface area and δ the skin depth. Maximizing the cavity volume to surface area ratio generally increases the Q, and thus discourages one from using cavities which are elongated in one direction. For a combination of all of the above reasons, we have chosen to use cylindrical resonant cavities operating in the TE_{011} mode [4], and with the exception of a brief digression in Section 2.1.2, we will limit our discussion to the properties of these cavities.

2.1.1 Cylindircal TE_{011} Cavity

The cylindrical cavities are fabricated from oxygen free copper (OFC) and consist of an annular cavity body on which two flat endplates are mechanically attached with screws. The field distributions within the cavity are shown in Figs. 1 and 2. In this mode only circumferential currents flow, both in the cylindrical walls and endplates, and thus both the field distribution and Q are virtually independent of the quality of the contact between the body-walls and the removable endplate (i.e. since no current flows between the wall and endplate). This feature allows one to open the cavity (e.g. to introduce the sample) without a subsequent degradation of the Q. Unfortunately, this mode is also degenerate with the TM_{111} mode. As the two modes have different field distributions, the degeneracy can be removed by slightly modifying the shape of the resonator. In our case, the mode splitting is accomplished by cutting small grooves at both the top and bottom edges of the cavity body, as shown in Fig. 3a. The grooves are at the position of an anti-node in the TM mode and a node in the TE mode. The net effect is that the TM mode sees an effectively larger cavity, thus shifting its resonance to lower frequencies.

The diameter d to height h ratio of the cavity is chosen in order to both optimize the Q of the TE_{011} mode (maximum with d/h near 1) while also minimizing the density of modes near the desired resonance frequency. A ratio $d/h \approx 1.50$ represents a good compromise between these conditions and as shown in Table 1, most of our cavities are near this ratio.

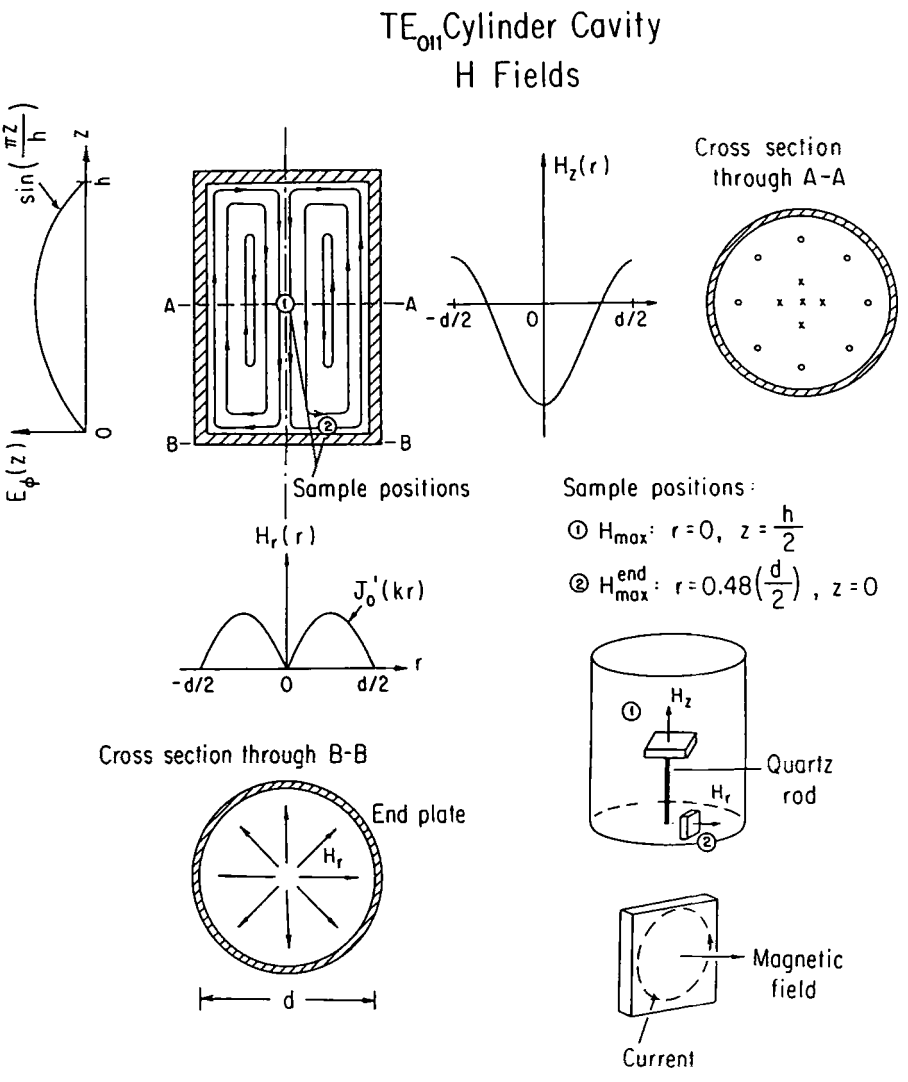

Figure 1: *Magnetic field lines inside a cylindrical cavity resonating in the* TE_{011} *mode. Both* H_{max}*, the maximum magnetic field in the cavity, position 1, and* H_{max}^{end}*, the maximum magnetic field on the endplate, position 2, are indicated on the figure.*

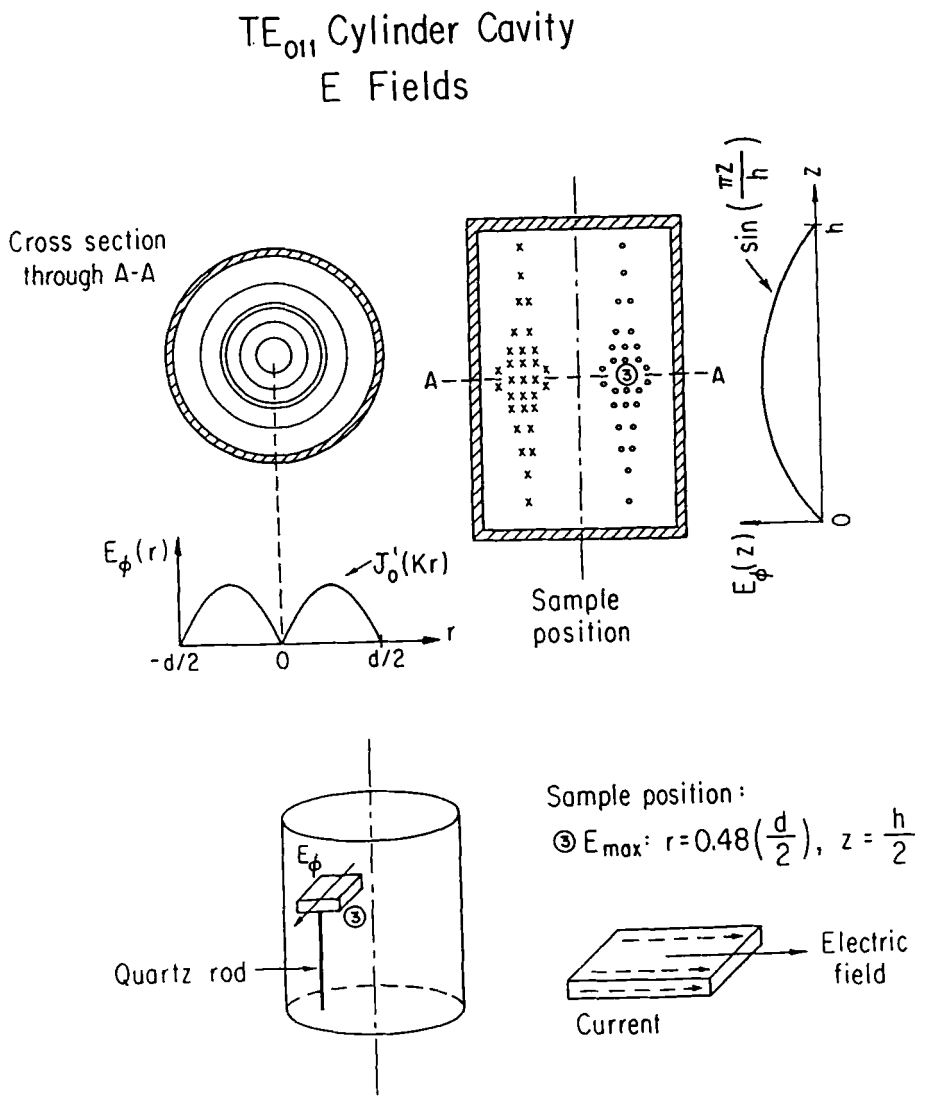

Figure 2: *Electric field lines inside a cylindrical cavity resonating in the* TE_{011} *mode. The position of the maximum electric field* E_{max}*, position 3, is indicated on the figure.*

Table 1: *The resonant frequency f_o, quality factor Q, diameter d, height h and volume V_c for each of our cavities in the micro and millimeter wave spectral range. At 3 GHz we have indicated the size of the split ring resonator, not the volume in which the fields are contained.*

f_o GHz	Q @ 300 K	d mm	h mm	V_c mm^3
3.0	2,000	10.00	25.4	1,995
7.5	20,000	57.28	38.19	98,411
9.2	25,000	43.90	39.20	59,334
12	15,000	35.8	23.87	24,027
35	13,000	12.44	7.90	960.2
60	7,500	7.15	4.77	191.5
100	7,000	4.21	2.81	39.1
150	4,000	2.86	1.91	12.3

Finally, as seen in Eq. (2), the maximum sensitivity is achieved by minimizing δ, the skin depth of the cavity. For this reason, all of our cavities are made of highly conducting OFC, which is subsequently annealed (48 hours at 200°C), acid etched, and then manually polished with alumina powder. All interior surfaces have a mirror finish and the effects of oxidation are reduced by repeating the polishing procedure every several months.

2.1.2 Split Ring Resonator

One disadvantage of using hollow resonators is that, as the cavity volume varies as ω_o^{-3}, they become very large at low frequencies. Therefore, for fixed sample size (unfortunately this is usually the case), the sensitivity S decreases as ω_o^3 (apart from any changes in the resonator constant or sample properties). In addition to the loss of sensitivity, the sheer physical size of the cavity makes it both difficult and expensive to reach low temperatures. For these reasons, a good deal of effort has been directed towards developing open-type resonators at low frequencies [4, 5]. In particular, the use of a resonator which works well at low frequencies (below 7 GHz) has been pioneered by W. Hardy and his associates [6, 7].

2.2 Coupling

Typically, the microwave power is directed from the source through a rectangular waveguide to the cavity. The excitation of a particular cavity mode is made by connecting a similar field pattern in both the waveguide and the cavity, as shown in Fig 3a. This can be accomplished with either a thin wire antenna or a small hole (coupling hole) in the cavity wall. A wire antenna, placed in the electric field maxima of the waveguide, can either couple di-

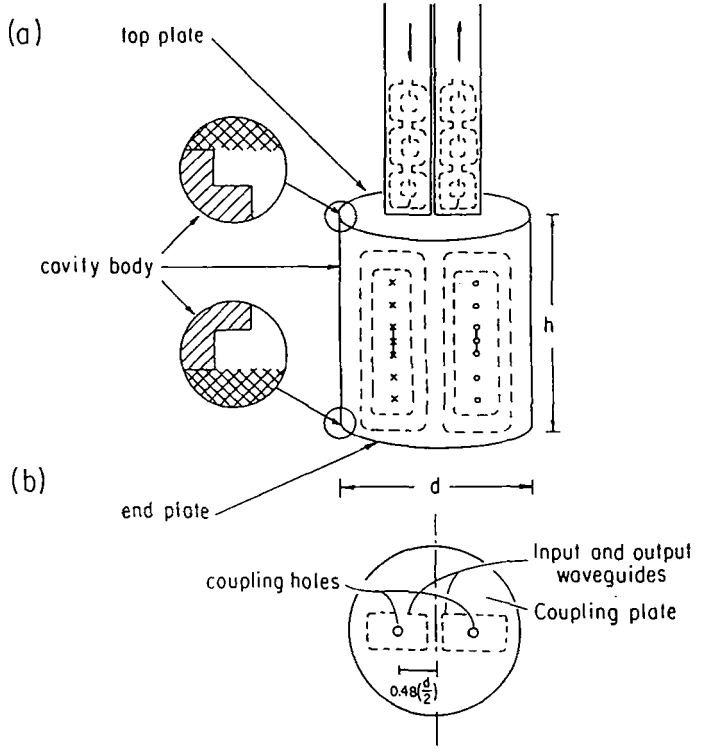

Figure 3: a) *Sideview of a* TE_{011} *cavity coupled via the magnetic field (dashed lines). The grooves in the cavity walls split the degenerate* TE_{011} *and* TM_{111} *modes by shifting the* TM_{111} *mode to lower frequencies.*
b) Cavity top plate used in a transmission configuration. The two coupling holes are centered about the position of the maximum magnetic field on the endplate, a distance of 0.48 times the cavity radius from the center. The waveguide is attached such that the coupling holes are at the position of the maximum magnetic field in the waveguide.

rectly to the electric field inside the cavity or it can be formed into a current loop, thus coupling to the magnetic field. On the other hand, a coupling hole at the terminating point of the waveguide is in an electric field node and can therefore only couple to the magnetic field inside the cavity.

The strength of the coupling is defined as the ratio of the absorbed power at the resonance frequency to the reflected power just off the resonance. The coupling strength can be adjusted by varying the size and/or shape of the device. Increasing the coupling increases the radiation loss, decreasing, see Eq. (3), the cavity Q and sensitivity S, while simultaneously increasing the signal to noise ratio. We typically use undercoupled cavities with a coupling near 0.1 to ensure a large Q and then average the detected signal several hundred times to increase the signal to noise ratio.

It has been found experimentally that coupling through a small hole in the cavity wall is much *less* temperature dependent than coupling with a wire antenna. This becomes particularly important when using the amplitude technique; we will describe this technique in detail in the following sections. For this reason, we couple, whenever possible, with a small hole in the top plate of the cavity. This hole is located at the position of the magnetic field antinode in both the waveguide and cavity. For a TE_{011} cylindrical cavity, the coupling hole is located at a point which is 48% of the cavity radius from the center, as shown in Fig. 3b. The waveguide is centered about this point and terminated with a 0.25 mm thick OFC coupling plate. The coupling hole diameter varies with the cavity resonance frequency, but the 0.6 mm diameter hole we use in our 100 GHz cavity is fairly typical.

3 Cavity Perturbation

Depending on the sample size and shape, different types of perturbations are made. In some cases a particular type of perturbation is chosen to maximize the measurement sensitivity, while in other cases the physical characteristics of the sample to be investigated dictate the arrangement. An isotropic sample of the appropriate size will give identical results for each of the following perturbation techniques. However, as the direction of the induced currents differs with each technique, anisotropic samples will generally give different results in each configuration.

3.1 Endplate Perturbation

If the sample dimensions exceed the cavity diameter in at least two directions the endplate can be replaced by the sample, as illustrated in Fig. 4. In this, the so-called endplate technique, certain other restrictions are placed on the physical properties of the sample:

- The sample thickness must exceed its skin (or penetration) depth in order that the cavity Q is not significantly altered by radiation losses through the endplate. Practically speaking, this limits the use of this type of a perturbation to highly conducting samples. Note, corrections for radiation leakage are difficult, one must include the effects of all materials (e.g. the sample substrate) near the cavity endplate, but sometimes possible [8].

- The sample conduction must be nearly isotropic in the plane of the endplate (i.e. at least a two-dimensional (2-D) conductor) as circumferential currents flow in the plane of the endplate (ϕ direction). Note, an in-plane anisotropy changes the field distribution and the cavity Q in a fashion which requires an *a priori* knowledge of the anisotropy. However, materials with a mild in-plane anisotropy (e.g. high temperature superconductors with an anisotropy of 2-5) have given results which are consistent with measurements made in other configurations [9, 10, 11].

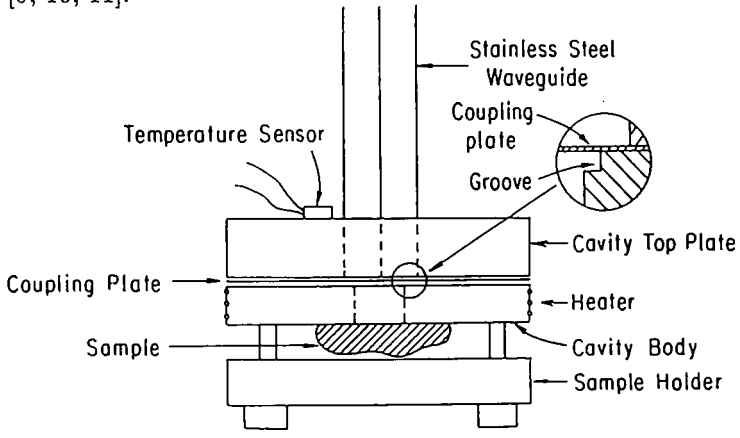

Figure 4: *Diagram of the setup used for the endplate perturbation. The endplate is replaced with the sample under investigation.*

- The sample has to be flat over a distance of the cavity diameter.
- The surface of the sample should be smooth down to the length scale of the skin-depth (or penetration depth).

With this configuration, the in-plane conductivity is measured and, unless the sample is large enough to polish several perpendicular faces, the anisotropy cannot be extracted.

3.2 Enclosed Perturbation

If the sample dimension is much smaller than the wavelength, one can introduce the sample inside the cavity. The maximum sensitivity is realized at the antinode of either the electric or magnetic field. The antinode positions, $H_{\max}$ and $E_{\max}$, are shown in Figs. 1 and 2 for a cavity in the TE_{011} mode. There are several important points to note:

- The direction of current flow within the sample differs at the electric and magnetic antinode. Combining the results from measurements in the two antinodes permits a direct measurement of the anisotropy. This is of particular importance in strongly anisotropic conductors.
- Unlike an endplate perturbation, there are no inherent limitations on the range of sample conductivity which can be measured. Ultimately, the range of sample conductivity which can be extracted depends only on the sensitivity of the measurement, and is determined by such factors as the sample size, shape, and location, and the cavity Q and resonance frequency f_o.

With both the endplate and enclosed perturbation techniques, the cavity must be opened to introduce the sample. This is usually accomplished by removing the endplate. The sample is then positioned atop a small quartz rod (diameter 0.2 mm and height $h/2$) which is glued to the endplate at the appropriate location of either $E_{\max}$ or $H_{\max}$ (see Figs. 1 and 2). The quartz rod does not significantly alter the cavity Q but does introduce a slight shift in the resonance frequency. However, as the quartz rod is present for both the unperturbed (o) and perturbed (s) measurements, this frequency shift does not affect the analysis in any way.

On the other hand, we have found that due to the extreme sensitivity to the cavity volume, it is not possible to remove and replace the endplate

without introducing an unreproducible frequency shift between the two runs [(o) and (s)]. The shift is due to the mechanical nature with which the endplate is fastened to the bottom of the cavity and in our 60 GHz cavity a shift of $\pm$ 2 MHz is typical (this corresponds to a change of $\pm$ 0.5μm in the cavity height). As this shift occurs between the two runs, it affects the subsequent analysis. We will come back to this problem in Section 6, where we will explain how in certain cases this frequency offset can be determined.

3.2.1 Electric Field

In the electric field antinode, position 3 on Fig. 2, the current flow is along the field direction, in the ϕ direction. If the maximum sample dimension is much less than the field radius of curvature, one can directly measure the conductivity along any desired direction by properly orienting the sample. However, it should be noted that the depolarization factor generally varies for each sample orientation and thus the corresponding measurement sensitivity is usually much different for measurements made in each direction.

3.2.2 Magnetic Field

In the magnetic field antinode, the inductive eddy current flows in a plane perpendicular to the field and the in-plane conductivity is measured. However, unlike with the endplate technique, the sample can be easily rotated to determine the conductivity in any desired plane, and, depending on the sample geometry and anisotropy ratio, one may be able to extract the conductivity along a particular direction.

One drawback of the enclosed cavity perturbation technique stems from the difficulty in accurately orienting the sample atop a thin quartz rod. However, for measurements in the magnetic field, this problem can be eased by placing the sample in the position of the field maximum on the endplate $H_{\mathrm{max}}^{\mathrm{end}}$, indicated as position 2 on Fig. 1. In this case the sample rests on the cavity endplate and can be easily manipulated. There are two important facts concerning measurements in $H_{\mathrm{max}}^{\mathrm{end}}$:

- In a TE_{011} mode, the magnetic field at this position is smaller by a factor of 4.18 h/d, thus decreasing the sensitivity of the measurement. With $h/d = 0.67$, the field is smaller by a factor of 2.8 and the sensitivity is reduced by a factor of almost 8 (see Part I).

- A conducting sample on the endplate alters the field distribution in the vicinity of the sample. This in turn changes the current distribution on the endplate and can cause a slight change in the loaded Q which does *not* originate from a loss in the sample. We have attempted to place an upper limit on the size of this effect by measuring a superconducting sample on the endplate. We have found that for small volume filling factors (typically 10^{-4} or less), this effect is negligible.

Since we are normally well above the sensitivity limit, a large advantage is realized by the comparative ease with which the sample can be manipulated on the endplate, and therefore this is the usual configuration used in our magnetic field measurements.

3.3 *Insitu* Perturbation

The major disadvantage of the enclosed perturbation is the unavoidable presence of a frequency offset which accompanies the opening of the cavity. One way to avoid this problem would be to mechanically introduce the sample through a small hole in the cavity. While such a technique would remove the unknown frequency offset, the additional hole in the cavity would serve to increase the radiation losses ($1/Q_r$). However, it is expected that at low frequencies, where the volume to surface area ratio of the cavity is large, such a hole would not drastically reduce the Q. For these reasons, we have, following a design by Buranov [12], fabricated several low frequency cavities (7, 9 and 12 GHz) which are designed to allow an *insitu* perturbation.

The modifications to the usual cavity design are as follows (Fig. 5): A thin slit is cut along the direction of the current flow in the cavity sidewall (ca. 2 mm wide and 25 mm long), large enough to pass a thin, symmetric (about the axis of rotation) Teflon sample holder. The holder is fastened to a quartz rod (diameter 1.1 mm) which is introduced into the cavity through a small hole in each endplate. The entire assembly is rotated with an externally mounted stepping motor such that a section of the Teflon holder passes through either the electric or magnetic field maximum.

The rotational symmetry of the Teflon sample holder is first checked so that both the resonance frequency and width are unchanged by a 180° rotation of the holder. The sample is then placed on one end of the holder while a thin gold wire is separately placed at the opposite end. The size and shape of the gold wire are chosen such that the frequency with the gold wire

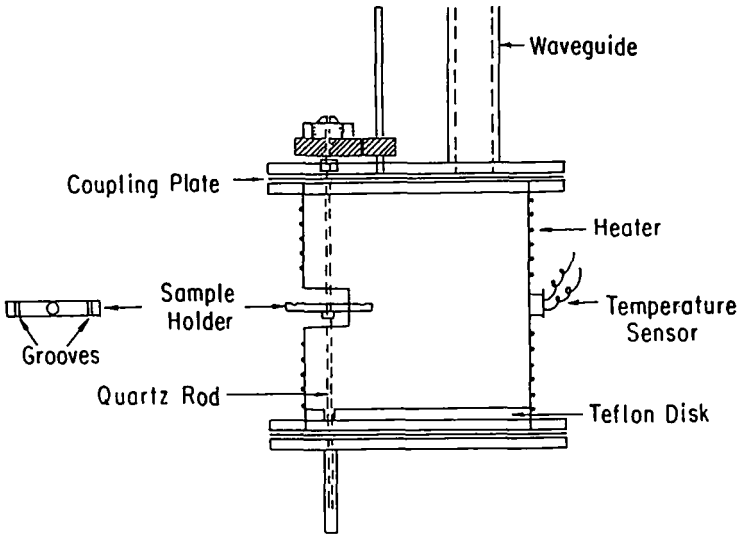

Figure 5: *Side view of a cylindrical cavity used for the* insitu *perturbation. The sample is placed in either of the grooves on the Teflon sample tray and in this configuration it will pass through* $E_{\max}$ *inside the cavity.*

inside the cavity matches that found when the sample is inside (i.e. $f_{\mathrm{Au}} = f_s$), while also minimizing the change in width from the unperturbed cavity (i.e. $\Gamma_o \approx \Gamma_{\mathrm{Au}}$). In this way, one can sweep through both resonances using only a narrow frequency sweep. We typically frequency balance $(f_s - F_{\mathrm{Au}})$ to within 1 MHz with only a 1% change in the width $(\Gamma_{\mathrm{Au}} - \Gamma_o)$ at room temperature.

4 Experimental Setup

4.1 Components

4.1.1 Sources

The microwave power is generated with a variety of different solid state devices. Below 20 GHz, a broad band oscillator is used which is filtered with a narrow band YIG cavity. At higher frequencies, either a Gunn diode (typically 1 GHz bandwidth) or an Impatt source (approximately 10 GHz bandwidth) is used. These are low noise and low power devices (less than

100 mW) which are readily available. In all cases, the sources are voltage controlled with the frequency proportional to the applied voltage.

4.1.2 Detectors

A variety of rectifying diodes with a dc output voltage which is proportional to the incident microwave power are commercially available. The response is typically found to be linear over 5 or more orders of magnitude in the incident power.

4.1.3 Temperature Regulation

The cavity temperature is monitored with a silicon diode mounted on the outer wall (see Fig. 4). A 50 Ω heater wire is wound around the exterior of the cavity and the temperature regulation is performed with a Lake Shore DRC-91C Temperature Controller. In this configuration we can measure from 1.2 K to 300 K with a thermal stability which is better than 10 mK.

Care has to be taken to avoid heating the sample with the microwaves (especially when it is mounted atop a quartz rod in the interior of the cavity) and we typically inject a small amount of He exchange gas inside the can to avoid this problem. Furthermore, we routinely test that the cavity width (with the sample inside) is independent of the incident power in order to ensure that the cavity and sample are at the same temperature.

4.2 Configuration

In all configurations discussed so far, the microwave cavity is mounted at the end of a rectangular stainless steel waveguide. This assembly is enclosed in a sealed copper can which bathes in liquid He. A Mylar window, in a section of the waveguide which remains at 300 K, provides a vacuum tight environment. The thermal link to the He bath is variable and originates from two main sources: thermal conduction down the stainless steel waveguide (fixed) and He exchange gas inside the can (variable). A weak bath/cavity thermal link is desirable as it allows one to vary the cavity temperature independently of the bath temperature. Typically we use a few Torr of He exchange gas in order to provide a reasonable compromise between the desire to maximize the sample/cavity thermal link while minimizing the bath/cavity link. One

of two different experimental configurations, the reflection or transmission mode, is used when making cavity perturbation measurements.

4.2.1 Transmission Mode

In the transmission mode, the microwave power is input through a coupling hole into the cavity, while the detection is made via a detector mounted atop a separate waveguide coupled to the cavity through a second hole. A typical transmission setup is shown in Fig. 6. The microwave power is directed through a ferrite isolator, a 10 dB directional coupler and a modulator. The reference arm of the 10 dB directional coupler is attached to either a reference cavity or a broadband mixer, which is in turn connected to a microwave frequency counter. The frequency counter is capable of reading frequencies up to 110 GHz. The modulator can chop the microwave power at frequencies up to 100 kHz, and is the only piece of equipment which must be added to a conventional setup in order to use the amplitude method described below. After passing through the cavity, the transmitted microwaves pass through another ferrite isolator before reaching a diode detector. The uni-directional ferrite isolators greatly reduce the amplitude of the standing waves in the waveguide and provide the main advantage of the transmission configuration.

4.2.2 Reflection Mode

In this mode, the incident microwave power reflected at the input coupling hole is detected via a circulator. In this way the power absorbed at the resonance is directly measured. Since only one cavity coupling hole is required, the radiation losses are reduced, thus increasing the cavity Q and the measurement sensitivity. Furthermore, only one waveguide must be connected to the cavity and, compared with the transmission setup, a better thermal isolation of the cavity is possible.

Unfortunately, in an undercoupled cavity nearly all the incident power is reflected and consequently, large standing waves are formed in the waveguide. Due to these standing waves, the amplitude of the detected signal is strongly frequency dependent and the detected absorption peak is seen to rest upon a periodically modulated baseline. In order to fit the absorption spectra, a baseline correction procedure is required. We have employed the following procedure: The measurement of the resonance resting upon the baseline is followed by a 90^o rotation of the sample holder. The rotation causes a

shift in the resonance frequency which must exceed the size of the frequency sweep (this places a condition on the maximum size of the frequency sweep), thus permitting a second measurement of only the baseline. Provided the rotation of the Teflon holder does not modify the standing wave pattern in the waveguide (not a problem provided a small holder is used), the difference of the two curves gives the cavity resonance and can be fit to a Lorentzian of the form of Eq. (20) of Part I.

It should be noted that in practice, this procedure can only be used at frequencies below 20 GHz as at higher frequencies the period of the baseline modulations become comparable to the width of the resonance itself.

5 Experimental Techniques

The experimental methods used in a cavity perturbation measurement vary somewhat, but in all cases, two separate measurements, one with the sample and one without it (in the case of the endplate technique a copper endplate replaces the sample), are performed at each temperature and, except for the *insitu* perturbation, two complete temperature sweeps must be made. Between the temperature sweeps, the cavity is opened and the sample is removed. The empty cavity is closed and the temperature cycle is repeated. In order to extract the cavity characteristics Γ and f_o, two different techniques are generally employed.

5.1 Width Technique

The most common method employed to measure f_o and Γ uses a broad sweep of the source frequency over a range which is at least several times the resonance width. The detected signal is amplified and then averaged (typically 100 times) with a digital oscilloscope before fitting with a Lorentz curve. A schematic diagram of the setup is shown in shown in Fig. 6.

There are several factors which complicate the measurement of the frequency. The resonant frequency f_o of the cavity is strongly temperature dependent (due to the thermal contraction of the cavity), and this requires one to either periodically adjust the source central frequency or to make a sweep which is larger than the shift caused by the thermal contraction of the cavity. Typically a change of 500 MHz to 2 GHz is seen in f_o between 1.2 K and 300 K, and such a large frequency sweep, together with the smearing of

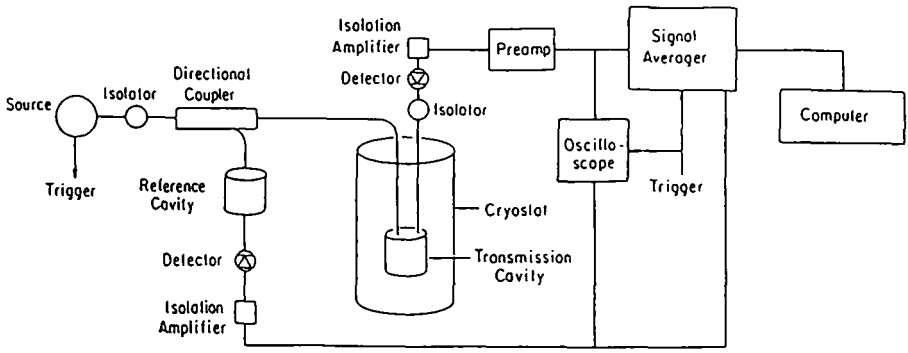

Figure 6: *Detection scheme used for measuring with the width method. The source is swept over a broad frequency range and the detected signal is fit to a Lorentzian curve with a computer.*

the peak due to the averaging, makes it difficult to attain a high precision measurement. Therefore, one of two standard techniques is commonly used to measure the frequency:

- A large frequency sweep is used and the absolute value of the frequency is set by a reference cavity at room temperature, connected to the source via a directional coupler. In this case, only the difference in frequency between the two cavities is needed, and therefore the frequency is measured to an accuracy which is in principle only a factor of two worse than the width. However, for large sweeps the approximation of a linear frequency-voltage response in the Gunn diode begins to break down and one must rely on a previous calibration of the diode response. It has been found experimentally that with this technique, the frequency is typically measured with a precision which is at least a factor of 5 smaller than the width.

- A narrow frequency sweep is employed (several half widths) permitting the use of a frequency counter to measure the source central frequency. In this case, the width is, as usual, determined solely from the fit, while the frequency is determined by the sum of the frequency fit parameter and the reading of the frequency counter. The two characteristics are thus determined independently from one another (i.e. the uncertainty of the frequency and width need not be the same). However, even under these conditions, the large long-time drift of the source frequency

leaves one with a frequency uncertainty which is as much as an order of magnitude larger than the width uncertainty.

5.2 Amplitude Technique

A more accurate way to measure both the bandwidth and the characteristic frequency in a cavity in the transmission mode uses a narrow frequency sweep about f_o while measuring the power transmitted at the resonance. As the sweep in frequency is typically orders of magnitude smaller than with the conventional method, the characteristic frequency can be directly measured with a frequency counter up to an arbitrary accuracy by appropriately averaging. The bandwidth is inversely related to the square of the power

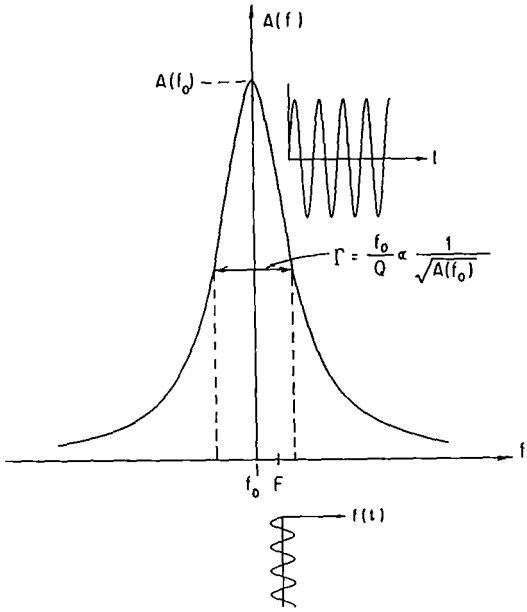

Figure 7: *The principle of the amplitude method detection scheme; a modulation frequency $f(t)$ ($|f| \ll \Gamma$) is superimposed on the central frequency F of the source. The in-phase component of the detected signal is proportional to the difference (F-f_o). This difference is fed back to the source as a correction, "locking" F to f_o. By accurately measuring F (e.g. with a frequency counter) and the amplitude of the signal at f_o, $A(f_o)$, one can deduce both f_o and Γ.*

absorbed at the resonance (the integral of the transmitted spectrum is proportional to the power of the source times $1/\Gamma$) and can thus be determined indirectly. Using this type of detection necessitates that the source central frequency is locked to the characteristic frequency of the resonator. This can be achieved with a feedback loop, in a fashion similar to that used in a standard FM radio. We refer to this measurement technique as the amplitude technique.

In order to lock on to the resonance, one must constantly minimize the difference between the central frequency of the source, F, and f_o (see Fig. 7). This can be achieved by periodically modulating, with period T, the source frequency by a small amount δF about F while making a phase sensitive detection of the in-phase component of the transmitted signal at the frequency $1/T$. The in-phase component measures the derivative of the absorption spectrum and, to first order, this is proportional to the error signal (F-f_o). This error signal is fed back to the source and constantly provides a correction to the source frequency. In this way the source frequency is locked to the cavity resonance frequency. With the above mentioned sources, F is proportional to the total dc voltage V_{dc} applied and changes of F in steps less than 1 ppm are possible. The total frequency of the source F_s is the sum of the central frequency F and the time dependent modulation $f(t)$

$$F_s = F + f(t). \tag{5}$$

The modulation, $f(t)$ is periodic (typically 10 ms) with an amplitude (approximately 0.1 MHz) which is less than 1% of the resonator bandwidth. A computer monitors the error voltage and adjusts F to minimize the feedback voltage, thus providing the large long term frequency shifts required to keep up with a strongly temperature dependent resonant frequency. This system is equivalent to the Automatic Frequency Control (AFC) in an ESR spectrometer. The short term integrator is set by the phase-sensitive detector and is on the order of a few seconds. The long term integration is done by an interfaced computer that periodically adjusts (few minutes period) the voltage V_{dc} to minimize the error signal. With this method we are able to measure directly the central source frequency with a frequency counter with an accuracy of $\pm$ 10 kHz, which is roughly 10 times better than with the conventional technique. For a more detailed discussion of the sensitivity of these measurements see Part III [13].

To measure the bandwidth, the emitted microwave power is chopped and the transmitted power is directly measured with an additional phase sensitive detector. A schematic diagram of the setup can be seen in Fig. 8.

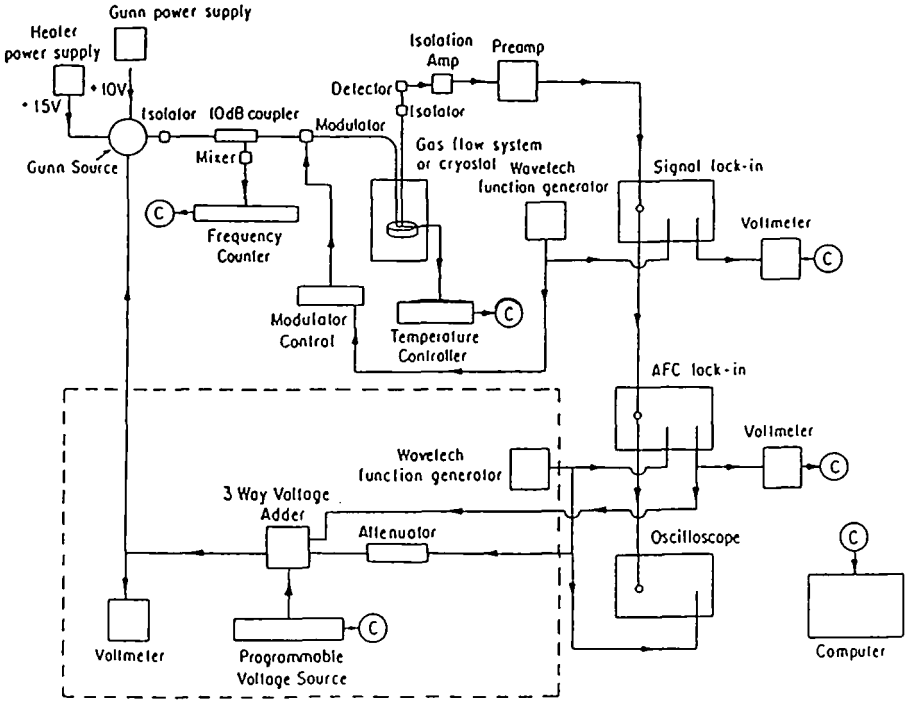

Figure 8: *Experimental setup for the amplitude measurement technique. This particular configuration is used with a varactor tuned Gunn oscillator. If an Impatt source is used, the elements within the dashed box are replaced by an HP 8350B sweep oscillator.*

The chopping frequency is near 10 kHz, far enough above the frequency $1/T$ to avoid mixing, yet well below the upper frequency limit of the modulator.

In the amplitude method one directly measures both f_o and the transmitted power at f_o, $A(f_o)$. For a Lorentzian response

$$A(f) = \frac{\zeta/4}{(f - f_o)^2 + \Gamma^2/4} \tag{6}$$

where $\zeta/4$ is a constant which depends on a variety of quantities, e.g. the source power, the coupling, and the attenuation. The power transmitted at

the resonance frequency is given by

$$A(f_o) = \zeta \Gamma^{-2}. \tag{7}$$

In Fig. 9 we show the measured width together with $1/\sqrt{A}$ over a broad temperature range. The good overall agreement confirms the validity of Eq. (7). As has been shown in Part I, the quantity of interest is $\Delta\Gamma$ which, using Eq. (7), is related to the measured values of $A_s = A(f_s)$ and $A_o = A(f_o)$ by

$$\Delta\Gamma = \Gamma_s - \Gamma_o = \left(\frac{\zeta_s}{\sqrt{A_s}} - \frac{\zeta_o}{\sqrt{A_o}}\right), \tag{8}$$

where ζ_s and ζ_o are the proportionality constants with the sample in and out of the cavity respectively. We have found that both ζ_s and ζ_o are virtually temperature independent over a broad temperature range and they are also unchanged by the introduction of the sample into the cavity. Thus, within the experimental accuracy, $\zeta_s = \zeta_o$, and Eq. (8) can be rewritten in the form

$$\Delta\Gamma = \Gamma_s - \Gamma_o = \zeta\left(\frac{1}{\sqrt{A_s}} - \frac{1}{\sqrt{A_o}}\right). \tag{9}$$

ζ is experimentally determined by measuring *both* the width and the amplitude at *one* temperature.

The fact that ζ is independent of both time and temperature has been checked experimentally on the scales needed for the experimental studies ($T < 100$ K and $t < 48$ hours). The independence of ζ implies the following:

1. The power of the source is constant over the time scale of days and that it is independent of frequency over a frequency range of approximately 50 MHz.

2. The coupling of the cavity is essentially unchanged over a broad temperature range.

3. The coupling constant is independent of the introduction of the sample into the cavity. This implies that the field distribution is not drastically changed once the sample is introduced.

These experimental facts are only true over a limited range of sample size. The validity of the above statements can be checked by measuring with both the width and amplitude method (see Fig. 9). This requires no physical modifications to the setup and one can easily switch from one method to the

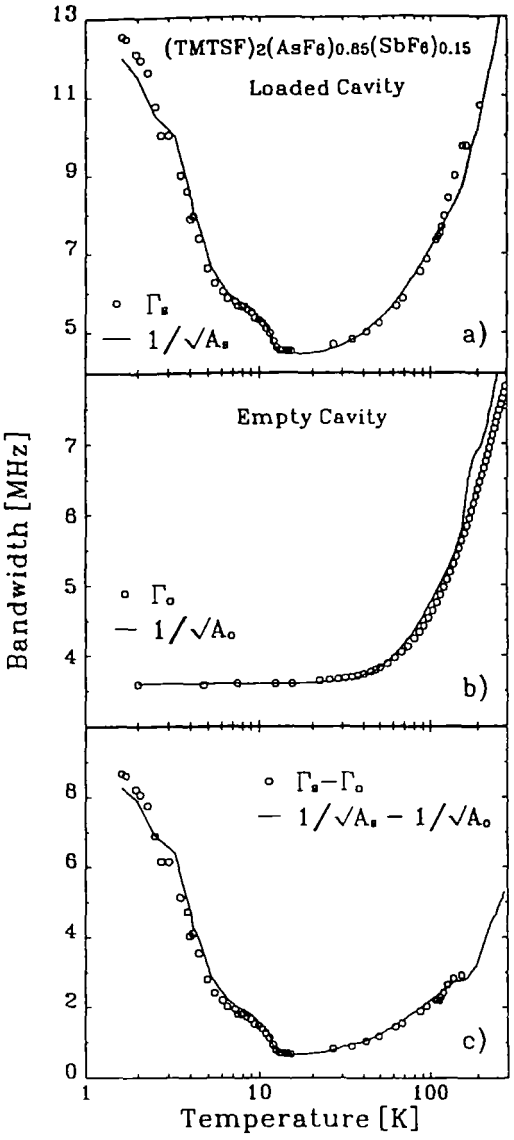

Figure 9: *Comparison of the temperature dependence of the bandwidth measured with the conventional width method (circles) and the amplitude technique (line) on a sample of* $(TMTSF)_2(AsF_6)_{0.85}(SbF_6)_{0.15}$ *at 60 GHz using an* insitu *perturbation. In a) the sample is loaded, in b) the cavity is empty, and c) is the difference between a) and b).*

other. Typically, we measure at several different temperatures using the width method, both with and without the sample. This is followed by a much more complete set of data taken with the amplitude method. The consistency is checked at the end by comparing the resultant width change using the two different configurations.

It should be noted that the amplitude of the transmitted signal is very sensitive to any absorption or radiative processes and care must be used to ensure the reproducibility of the measurement. In particular, when the cavity is opened to remove the sample one must consider the reproducibility of the following factors: quantity of exchange gas, liquid He levels, and the waveguide flange connections.

6 Data Analysis

6.1 Enclosed Perturbation

As the endplate removal does not (within experimental uncertainty) change the cavity Q, the analysis used to determine the width change for an enclosed perturbation is trivial. As shown above in Eq. (9), one simply takes the difference of the width with the sample in and out.

However, as mentioned previously, if the endplate is removed the frequency shift f_s - f_o can be measured only up to a numerical additive constant f_a. In this case, one finds

$$\frac{\Delta\hat{\omega}}{\omega_o} - \frac{f_a}{f_o} = \xi\hat{Z}_s. \tag{10}$$

f_a can be large (on the scale of say $\Delta\Gamma$) and cannot simply be ignored. An evaluation of this offset is possible in either of the two following cases:

1. If the sample is a simple metal then it can be shown that

$$\frac{X_s}{R_s} = \left(\frac{+\omega\tau + \sqrt{1+(\omega\tau)^2}}{-\omega\tau + \sqrt{1+(\omega\tau)^2}}\right)^{1/2} \approx 1 + \omega\tau + \frac{(\omega\tau)^2}{2} + \mathcal{O}[(\omega\tau)^3]. \tag{11}$$

In the so-called Hagen-Rubens limit, $\omega\tau \ll 1$ and $R_s = X_s$. Thus, from the measured surface impedance R_s, the surface reactance X_s can be determined and from Eq. (10) this is related to the unknown frequency shift f_a.

2. The sample is in a superconducting state of known penetration depth λ. In this case $\sigma_2 \gg \sigma_1$, $R_s \approx 0$, and $X_s = \omega\lambda/c_o$ and again, from a known value of X_s one can extract the frequency offset.

If none of these conditions can be fulfilled, it is not possible to isolate the part of the measured frequency shift due to the sample.

6.2 Endplate Perturbation

The case of the endplate perturbation is somewhat more complicated. In this type of a perturbation, one does not measure the perturbation due to the sample, but rather the difference in the measured width between the sample and copper endplates. The frequency of resonance f_o and the half-width Γ are measured as a function of the temperature in two separate runs, one before and one after the replacement of the copper endplate by the sample:

$$\Delta\Gamma = \Gamma_s - \Gamma_{\mathrm{Cu}} = \zeta\left(\frac{1}{\sqrt{A_s}} - \frac{1}{\sqrt{A_{\mathrm{Cu}}}}\right) \tag{12}$$

and

$$\Delta f = f_s - f_{\mathrm{Cu}} + f_a. \tag{13}$$

The difference is related to $\hat{Z}_s$, the surface impedance of the sample, through the relation:

$$\frac{\Delta\hat{\omega}}{\omega_o} - \frac{f_a}{f_o} = \frac{\Delta f}{f_o} - \frac{f_a}{f_o} + i\frac{\Delta\Gamma}{2f_o} = \xi(\hat{Z}_s - \hat{Z}_{\mathrm{Cu}}) \tag{14}$$

where $\hat{Z}_{\mathrm{Cu}}$ is the surface impedance of the copper endplate only and ξ is the resonator constant, given by

$$\xi = \frac{-ic_o^3\pi^2}{h^3\omega^3}. \tag{15}$$

In order to extract $\hat{Z}_s$, we use one of the following procedures. The surface impedance of the copper endplate can be determined with three different methods:

1. If the temperature is not too low then the surface impedance of copper can easily be obtained by assuming a simple Drude metal in the Hagen-Rubens limit. However, at low temperatures, the mean free path exceeds the skin depth (the anomalous regime) and such a simple expression is no longer valid.

2. One can calculate the ratio of the losses due to the copper endplate compared with the total losses at all the other surfaces in the cavity. This ratio is independent of the surface impedance. For a cylindrical cavity operating in the TE_{011} mode with a d/h ratio of 1.5, 39% of the wall losses occur on the endplate. If the assumption is made that all of the loses in the cavity occur at the walls of the cavity (i.e. neglecting coupling and radiation losses) then using Eq. (14) together with

$$\xi \hat{Z}_{\mathrm{Cu}} = 0.39 \frac{\hat{\omega}_{\mathrm{Cu}}}{\omega_o} \tag{16}$$

gives

$$\frac{\hat{\omega}_s - 0.61\hat{\omega}_{\mathrm{Cu}}}{\omega_o} - \frac{f_a}{f_o} = \xi \hat{Z}_s. \tag{17}$$

3. If a superconducting endplate of Nb is used then at low temperatures no temperature dependence is seen in the width. At this point one can assume that all the losses are coming from the copper walls. A second measurement with the copper endplate gives the additional losses due to this endplate.

From our experience, the third method is the most reliable. A typical value for copper at 100 GHz and 4.2 K is $R_s \approx 30\mathrm{m}\Omega/377\Omega \approx 7.96 \times 10^{-5}$. In order to determine $\hat{Z}_s$, the frequency offset f_a is evaluated as shown above for the enclosed perturbation.

6.3 *Insitu* Perturbation

In this case, the endplate is not removed and one need not worry about an unreproducible shift. However, the corrections due to the gold wire used to balance the holder must be included. In this case, one can exactly calibrate the device by separately measuring the frequency offset (and loss) of the gold wire.

7 Conclusion

In this paper we have discussed some of the experimental aspects of cavity perturbation measurements. In particular, we have described in detail several different methods each of which can be advantageous depending on the

sample to be measured. Furthermore, we have discussed the improvements we have made to the standard techniques which allow for a more precise determination of both cavity characteristics.

Acknowledgements

We wish to thank Dr. L. Drabeck for useful discussions and for letting us reproduced several illustrations from his thesis [14]. This research was partially supported by the INCOR program of the University of California. One of us (M.D.) would like to acknowledge the support of the Alexander von Humboldt-Foundation.

References

[1] F. Wooten, *Optical Properties of Solids* (Academic Press, San Diego, 1972).

[2] O. Klein, S. Donovan, M. Dressel, and G. Grüner, *Int. J. Infrared and Millimeter Waves* **14** (1993) (preceding article).

[3] J. D. Jackson, *Classical Electrodynamics* (John Wiley & Sons, New York, 1975).

[4] C. P. Poole, *Electron Spin Resonance* (Interscience, New York, 1975), p. 296.

[5] C. G. Montgomery, *Principles of Microwave Circuits* (McGraw-Hill, New York, 1948).

[6] D. A. Bonn, D. C. Morgan, and W. N. Hardy, *Rev. Sci. Instrum.* **62**, 1819 (1991).

[7] W. N. Hardy and L. A. Whitehead, *Rev. Sci. Instrum.* **52**, 213 (1981).

[8] L. Drabeck, K. Holczer, G. Grüner, and D. J. Scalapino, *J. Appl. Phys.* **68**, 892 (1990).

[9] O. Klein, K. Holczer, G. Grüner, and G. A. Emelchenko, *J. de Phys. I (France)* **2**, 517 (1992).

[10] L. Drabeck, K. Holczer, G. Grüner, J. J. Chang, D. J. Scalapino, A. Inam, X. D. Wu, L. Nazar, and T. Venkatesan, *Phys. Rev. B* **42**, 10020 (1990).

[11] One dimensional conductors have been measured in an endplate configuration on a rectangular cavity, T. Csiba, A. Blank, and G. Grüner (to be published).

[12] L. I. Buranov and I. F. Shchegolev, *Instrum. & Exp. Tech.* **14**, 528 (1971).

[13] M. Dressel, S. Donovan, O. Klein, and G. Grüner, *Int. J. Infrared and Millimeter Waves* **14** (1993) (subsequent article).

[14] L. Drabeck, *Surface Impedance of the High Temperature Superconductors* (Ph.D. thesis, UCLA, 1991).